Synthesis and characterization of Pr substituted Gd-123 high-T_c superconductors

(Síntese e caracterização de supercondutores de alta temperatura crítica $Gd_{1-x}Pr_x$-123, x=0/0,1/0,2/0,3)

V. R. Huse[1], V. D. Mote[1], Y. Purushotham[2], B. N. Dole[1]
[1]Materials Research Laboratory, Department of Physics, Dr. Babasaheb Ambedkar Marathwada University, Aurangabad - 431 004, India
[2]Centre for Materials for Electronics Technology, HCL (PO), Cherlapally, Hyderabad - 500 051, India
dolebn_phys@yahoo.in

Abstract

High T_c superconducting materials with chemical formula $Gd_{1-x}Pr_xBa_2Cu_3O_{7-\delta}$, where x = 0.0, 0.1, 0.2 and 0.3 were prepared by ceramic route. XRD studies confirm the orthorhombic pervoskite structure. Electrical resistivity measurement shows that T_c decreases with increasing Pr concentration. Copper valency and oxygen content decreasing with increasing Pr content. Value of $n(CuO_2)$ decreases with increasing x and oxygen deficiency (δ) has a linear dependence with (2x+δ). SQUID investigation reveals that Bohr magneton number and Curie constant are decreasing with increasing Pr concentration. Annihilation of superconductivity may be owing to reduction in CuO_2 charge carriers or magnetic pair breaking.

Keywords: Gd-123 HTSC, oxygen content, electrical resistivity, Curie–Weiss law.

Resumo

Materiais supercondutores de alta temperatura crítica com fórmula química $Gd_{1-x}Pr_xBa_2Cu_3O_{7-\delta}$, x = 0/0,1/0,2/0,3 foram preparados pela rota cerâmica. Estudos de difração de raios X confirmam a estrutura perovskita ortorrômbica. Medidas de resistividade elétrica mostram que T_C diminui com o aumento da concentração de Pr. A valência do cobre e o teor de oxigênio diminuem com o aumento do teor de praseodímio. O valor de $n(CuO_2)$ diminui com o aumento de x e a deficiência de oxigênio δ tem uma dependência linear com (2x+δ). Pesquisas em SQUID revelam qu o número do magneton de Bohr e a constante de Curie diminuem com o aumento da concentração de praseodímio. A aniquilação da supercondutividade pode ser devida à redução de portadores de carga em CuO_2 ou quebra magnética dos pares.

***Palavras-chave**: Gd-123 HTSC, teor de oxigênio, resistividade elétrica, lei de Curie-Weiss.*

INTRODUCTION

Tremendous efforts have been made to elaborate the mechanism responsible for superconductivity in oxide high temperature superconductors namely $REBa_2Cu_3O_{7-\delta}$ where RE is rare earth elements except Ce, Pr, Pm and Tb. Rare earth substitution for Y in $YBa_2Cu_3O_{7-\delta}$ gives rise to superconductivity with crit ical temperature T_c = 90 K and shows no affect on transition temperature, crystal structure and normal properties [1-6]. These materials are metallic and have an orthorhombic layered pervoskite structure. However, interesting exception is that $PrBa_2Cu_3O_{7-\delta}$ (Pr-123) crystallizes in the $YBa_2Cu_3O_{7-\delta}$ orthorhombic crystal structure and does not show superconductivity, it is an insulator instead of superconductor [7-9]. Extensive studies have been carried out to elucidate the mechanism responsible for the disappearance of the superconductivity in Pr-123 system [10]. The suppression of superconductivity in $REBa_2Cu_3O_{7-\delta}$ series is due to the partial substitution of Pr for the RE element [11-13]. Also found that Pr can be easily substituted without affecting the orthorhombic structure, but reduces superconductivity monotonically [14-16]. It is attributed by two mechanisms; first mechanism is filling of mobile holes in CuO_2 planes due to the substitution of Pr ions with a valence greater than +3 and hence implies that the suppression of superconductivity results from a reduced number of carriers in the CuO_2 sheets [17-19]. The second mechanism is pair breaking due to spin dependent exchange scattering of mobile holes in the CuO_2 valence band by Pr ions. Such large exchange interaction could be generated by hybridization of the localized Pr 4f states and adjacent CuO_2 valence band states. The origin of disappearance of superconductivity due to Pr substitution has not been well understood yet, although many researchers studied these problems. In spite of this substantial amount of investigation, interpretation for the mechanism responsible for GdPr-123 high temperature superconducting compound is not outlined yet.

However, Pr has different valence states of Pr_2O_3 (3+), PrO_2 (4+) and Pr_6O_{11} (3.7+). The partial presence of Pr ions in their trivalent state helps to stabilize the 123 phase structure. Hence in the case of Pr under the usual condition of synthesis, the 123 phase structure dominates. Since Pr is the only rare earth which can form the magnetic insulator Pr-123 instead of superconductor, with a structure isomorphic to the 123 phase which prevents complexities of structural changes. Partial substitution of Pr for Gd in Gd-123 can reveal valuable information on superconductivity and provides an opportunity for systematically studying the suppression of superconductivity and metal insulator transition.

In view of the above, a series with chemical composition $Gd_{1-x}Pr_xBa_2Cu_3O_{7-\delta,}$ where x = 0.0, 0.1, 0.2 and 0.3 were prepared to throw some more light to understand the mechanism responsible for superconductivity. X-ray diffraction was carried out at temperature for determination of structural parameters. SQUID measurements were performed for the evaluation of Bohr magneton and Curie constant.

EXPERIMENTAL

Samples with chemical composition $Gd_{1-x}Pr_xBa_2Cu_3O_{7-\delta,}$ where x = 0.0, 0.1, 0.2 and 0.3 were prepared by ceramic route. High purity powders Gd_2O_3, $BaCO_3$, Pr_6O_{11} and CuO (Aldrich make, 99.99%) were used stoichiometrically. The powders were mixed thoroughly, ground for 3 h and calcined at 915 °C for 24 h in air atmosphere. The calcination was repeated twice at 915 °C for 24 h for each with intermediate grinding for 3 h. Calcined samples reground for 2 h, then pressed into pellets using automatic press machine and sintered at 930 °C for 24 h. All samples were annealed in oxygen atmosphere at 450 °C for 24 h followed by slow cooling at 1 °C/min. up to room temperature.

Structural parameters were investigated using X-ray diffractometer (PW-3710) employing Cuk$_\alpha$ radiation (λ = 1.5418 Å). Electrical resistivity of the samples was measured in the temperature range 300 K to 4 K by dc four probe technique using a Physical Property Measurement System (PPMS). Magnetization was measured by a Quantum Design's Magnetic Property Measurement System (MPMS). The magnetic field 3 kOe was used to measure the susceptibility above T_C from which the Curie-Weiss parameters were obtained.

RESULTS AND DISCUSSION

XRD study

X-ray diffraction patterns of all the samples are shown in Fig. 1. It is evident from the figure that all samples have an orthorhombic perovskite structure without impurity phases.

The lattice parameters of all the samples were calculated using the formula:

$$d_{hkl} = \frac{1}{\sqrt{\frac{h^2}{a^2}+\frac{k^2}{b^2}+\frac{l^2}{c^2}}} \qquad \text{(A)}$$

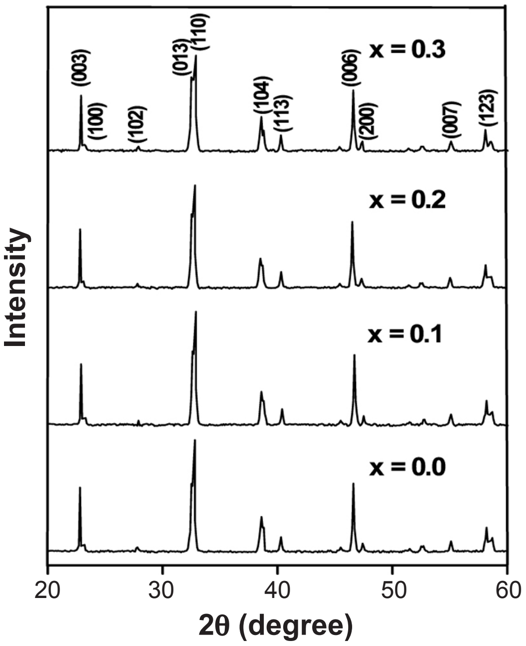

Figure1: XRD patterns of $Gd_{1-x}Pr_xBa_2Cu_3O_{7-\delta}$ system with x = 0.0, 0.1, 0.2 and 0.3.

[Figura 1: Difratogramas de raios X de $Gd_{1-x}Pr_xBa_2Cu_3O_{7-\delta}$ com x = 0/0,1/0,2/0,3.]

where, a, b, c are lattice parameters and (h k l) are Miller indices.

Variation of lattice parameters with Pr concentration is shown in Fig. 2. The lattice parameters 'a' and 'b' are increasing with respect to Pr concentration while the lattice parameter 'c/3' is increasing gradually and nearly constant ranging between 3.8906 Å to 3.8980 Å. It is interesting to note that the crystal structure remains nearly the same in all the samples. Hence, the unusual properties of the Pr doped Gd-123 system are not associated with a changing of the crystal.

Oxygen content plays an important role in assigning the orthorhombic to tetragonal structure in high temperature

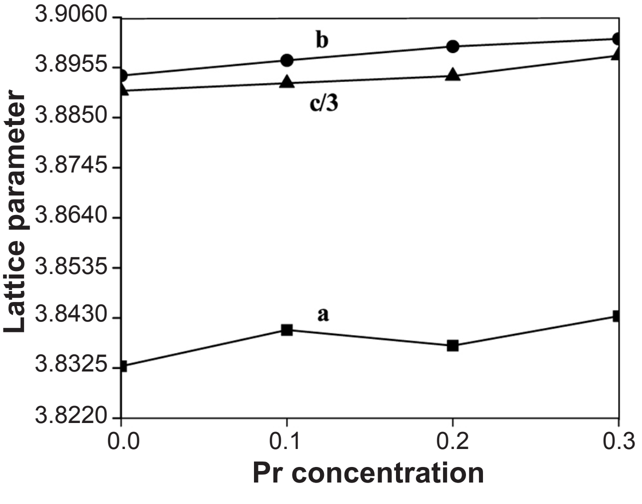

Figure 2: Lattice parameters vs Pr concentration.

[Figura 2: Parâmetro de rede em função da concentração de Pr.]

superconductivity. The stoichiometry δ = 0.00 is only reached if samples are slowly cooled at ambient temperature in oxygen atmosphere [20, 21]. The oxygen content for all the samples calculated using the formula [22]:

$$\delta = \frac{\frac{C_{exp}}{3} - 3.890}{0.047} \qquad \text{(B)}$$

Oxygen content and its variation with Pr concentration are shown in Fig. 3. The average oxygen content is found ~ 6.92 for all samples with minimum value 6.83 and maximum value 6.99. It is observed that the oxygen content depends on the lattice parameter 'c' and is independent for Pr content and hence the oxygen content remains almost constant for all x values. The orthorhombic distortion was evaluated using XRD data by the formula [c/(a+b)] [23] and its variation with Pr content is shown in Fig. 4. Orthorhombic distortion decreases drastically for x = 0.1, and for x = 0.2 and 0.3 it is almost constant. Hence, for the whole x range the system remains orthorhombic, but there is a tendency towards the tetragonal symmetry.

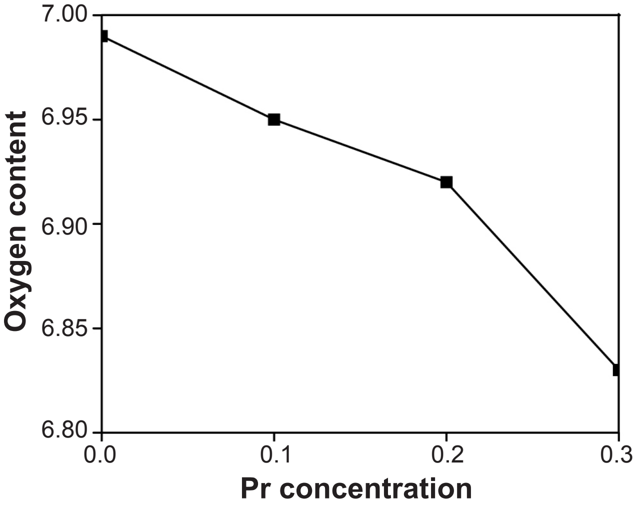

Figure 3: Oxygen content as a function of Pr concentration.
[Figura 3: Teor de oxigênio em função da concentração de Pr.]

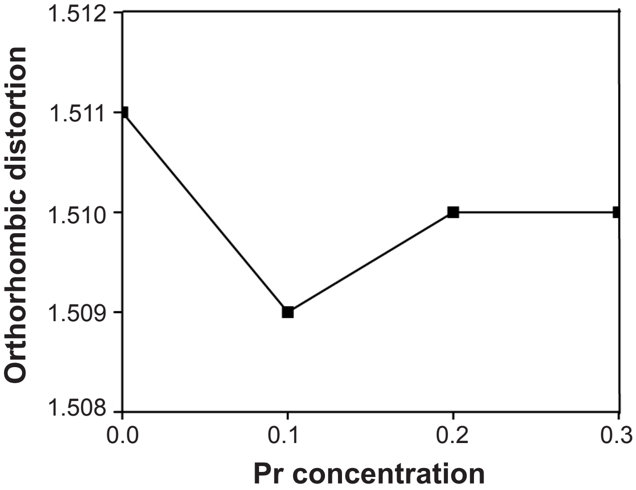

Figure 4: Orthorhombic distorsion as a function of Pr concentration.
[Figura 4: Orthorhombic distorsion vs Pr concentration.]

The superconducting properties of Pr substituted compounds are strongly dependent on structural changes that influence the Cu valence, thereby the number of holes in the CuO_2 planes [24] and on the oxygen defects ordering properties in the basal plane [25]. It has been established that holes are superconducting elements in p-type high T_c superconductors [26]. It is observed that the transition temperature of high cuprate superconductors fully depend upon holes as charge carriers.

The average charge 'p' per $[Cu\text{-}O]^{+p}$ unit or Cu valence is determined for all the samples using the formula [27]:

$$p = \frac{1 - 2\delta\ (Q_{Pr}\text{-}3)x}{3} \qquad \text{(C)}$$

and variation of copper valence with Pr concentration is shown in Fig. 5. It can be seen from the figure that the copper valence decreases with increasing Pr content following similar trend that of oxygen content as shown in Fig. 3. This shows that charge on [Cu-O] plane depends upon the Pr concentration as well as oxygen content in the sample. From this, one may conclude that for small p, the charge resides on the chains and these hole states are localized giving rise to an activated conductivity among the holes in the chains. At $x \geq 0.4$, $p > 0$, it does not show superconductivity in the sample because it may be due to the holes in the sheets and the inter basal planes are insulating. This shows that all of the $[Cu\text{-}O]^{+p}$ charge or holes must be in the inter basal plane. As the charge p increases at $x < 0.4$, the metallic conductivity and superconductivity occurs. This may be due to the increased charge which begins to appear on the sheet which can sustain superconductivity. This shows that the charge in the inter basal plane cannot be increased beyond the threshold value, a point at which charge begins to appear on sheet which can sustain metallic conductivity and superconductivity, so that

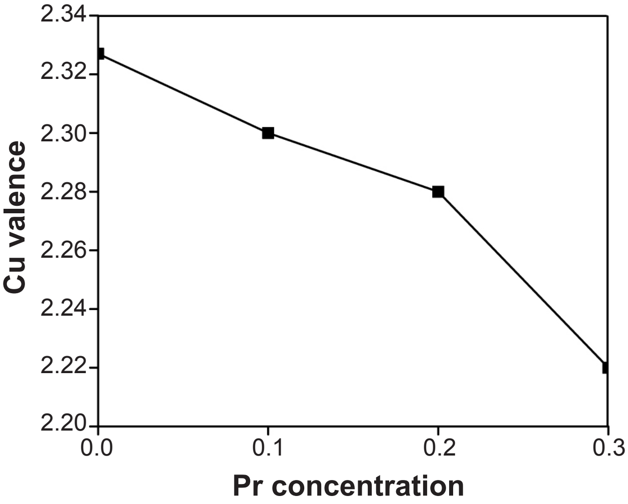

Figure 5: Copper valence as a function of Pr concentration.
[Figura 5: Valência do cobre em função da concentração de Pr.]

beyond threshold all increased charges come from the sheet.

Fig. 6 shows the variation of average charge 'p' per $[Cu\text{-}O]^{+p}$ unit versus oxygen content. It is observed that the charge (p) decreases with decreasing oxygen content. The reduction in the oxygen content lowers the number of oxygen atoms in Cu-O chains in the unit cell. There is a tendency for the oxygen atom vacancies to occupy a single chain [28]. As the oxygen content reduces from $7\text{-}\delta = 7$ to $7\text{-}\delta = 6$, then the oxygen vacancies are introduced in the CuO chain [29-31] and oxygen atoms completely vanished from the chain at $7\text{-}\delta = 6$. When $\delta = 1$, there are no chains and destruction of superconductivity occurs. In RE-123 compounds, the charge balance equation of the molecules for RE^{3+}, Ba^{2+} and $Cu^{(2+\delta)+}$ leads to $p = 0.33$ at $7\text{-}\delta = 7$. This excess amount of positive charge is responsible for superconductivity. From these results, one can say that the oxygen deficiency decreases the positive charges in CuO chain owing to the destruction of superconductivity.

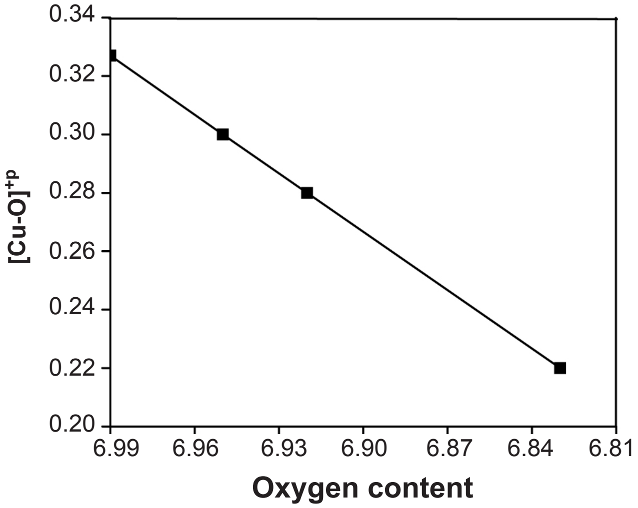

Figure 6: Average charge p per $[CuO]^{+p}$ unit as a fucntion of the oxygen content of $Gd_{1-x}Pr_xBa_2Cu_3O_{7-\delta}$ system.
[Figure 6: Carga média por unidade de$[CuO]^{+p}$ *em função do teor de oxigênio em* $Gd_{1-x}Pr_xBa_2Cu_3O_{7-\delta}$ *.]*

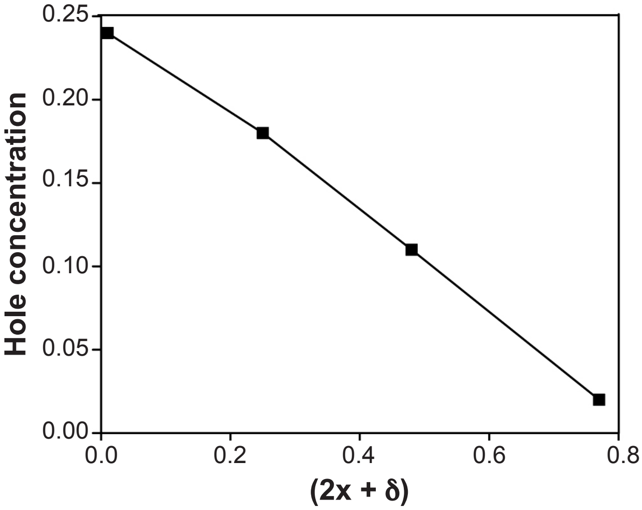

Figure 7: Hole concentration in CuO_2 plane vs $(2x+\delta)$.
[Figura 7: Concentação de buracosno plano CuO_2 *versus* $(2x+\delta)$*.]*

Hole concentration in the (CuO_2) plane against $(2x+\delta)$ is shown in Fig. 7. The value of $n(CuO_2)$ for optimum doping is 0.24 and is in good agreement with the reported literature [32, 33]. The value of $n(CuO_2)$ decreases with increasing x and δ and it has a linear dependence with $(2x+\delta)$. The decrement of hole concentration in the (CuO_2) plane is due to Pr doping which has mixed valency between 3+ and 4+ [33-36]. It implies that suppression of superconductivity results from a reduced number of carriers in the CuO_2 sheets and magnetic pair breaking effect.

Resistivity measurement

The electrical resistance of all samples measured in the temperature range 300 K to 4 K and its variation with temperature is shown in Fig. 8. The onset transition temperature ($T_{C(onset)}$), transition temperature at zero ($T_{C(0)}$) and transition width [$\Delta T_C = T_{C(onset)} - T_{C(0)}$] are tabulated in Table I.

Table I - $T_{C(onset)}$, $T_{C(0)}$ and ΔT_C of $Gd_{1-x}Pr_xBa_2Cu_3O_{7-\delta}$ system.
[Tabela I - $T_{C(onset)}$, $T_{C(0)}$ *e* ΔT_C *em* $Gd_{1-x}Pr_xBa_2Cu_3O_{7-\delta}$*.]*

Conc. (x)	$T_{C(onset)}$ (K)	$T_{C(0)}$ (K)	ΔT_C (K)
0.0	92.7	91.2	1.5
0.1	75.4	72.1	3.3
0.2	62.6	58.4	4.2
0.3	42.7	35.2	7.5

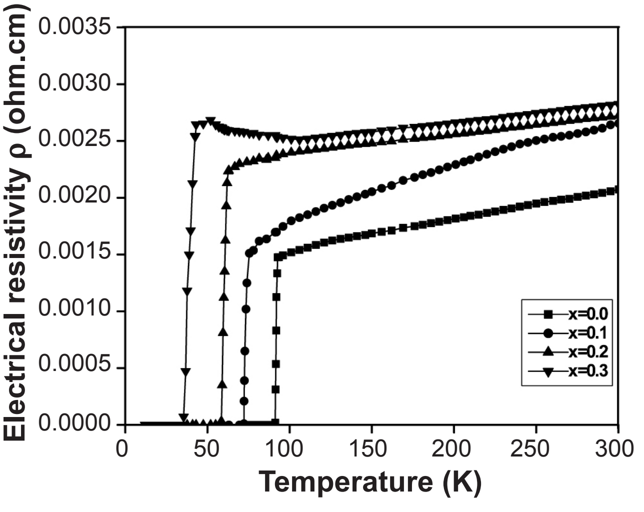

Figure 8: Electrical resistivity ρ as a function of the absolute temperature.
[Figura 8: Resistividade elétrica ρ em função da temperatura absoluta.]

The transition temperature T_C vs Pr concentration is shown in Fig. 9. It can be seen from the figure that T_C is decreasing with increasing Pr concentration. It shows that the Pr concentration, carrier concentration and T_C are closely related to each other. One can conclude that Pr doping reduces the carrier concentration either by hole filling or hole localization, due to hybridization of the Pr ion with the sandwiching CuO_2 planes, in a quantitatively similar way with oxygen depletion. In addition, the changes in the band structure related to the Pr substitution and hybridization of Pr 4f electrons with CuO_2 valence band decreases the T_C of superconductors. The results of electrical resistivity also reveal the larger influence of Pr substitution on superconducting transition temperature. It is also observed that $T_{C(onset)}$ varies linearly with $(2x+\delta)$. This linear behavior shows that there is a correlation between Pr concentration, oxygen deficiency and transition temperature T_C. It is observed that the depression of T_C in GdPr-123 is stronger than YPr-123 [11]. It may be due to the exchange interaction which is strengthened between hybridization of Pr and Gd 4f electrons because, ionic radius of Gd^{3+} is larger than that of Y^{3+}.

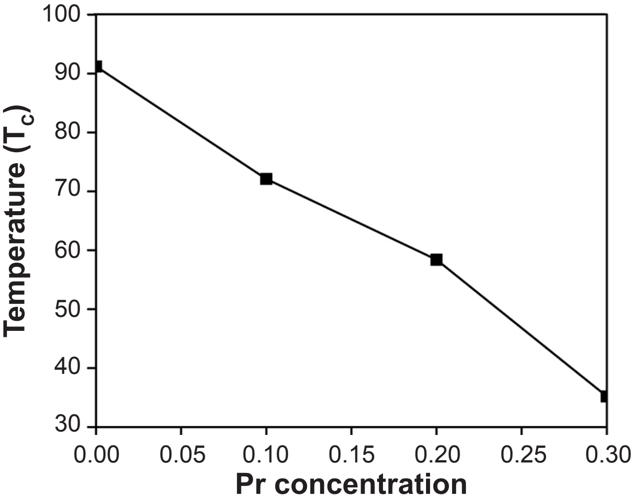

Figure 9: Transition temperature vs Pr concentration.
[Figure 9: Temperatura de transição versus concentração de Pr.]

Magnetic measurement

The molar susceptibility of all samples measured in the temperature range 300 K to 100 K using magnetic field 3 kOe by SQUID. The inverse magnetic susceptibility χ^{-1} vs T is shown in Fig. 10. Magnetic susceptibility decreases with increasing Pr concentration and obeys Curie-Weiss law [37, 38].

$$\chi = \chi_0 + \frac{C}{T - \theta} \qquad \text{(D)}$$

in which χ_o is Pauli-like susceptibility, θ is Curie-Weiss temperature and C is Curie-Weiss constant. The temperature independent susceptibility χ_o and Curie-Weiss temperature θ are only weakly concentration dependent. The μ_{eff} Bohr magneton number should be the resultant of the contribution from both Pr and Gd ions if the contribution from Cu ions is neglected. The experimentally determined Bohr magneton number value is approximately equal to the theoretical counterpart as estimated by the formula [37]:

$$\mu_{eff} = \sqrt{\frac{3K_BC}{N}} \qquad \text{(E)}$$

where K_B (Boltzmann constant) = 1.38×10^{-16} erg/K and N (Avogadro's number) = 6.02×10^{23}.

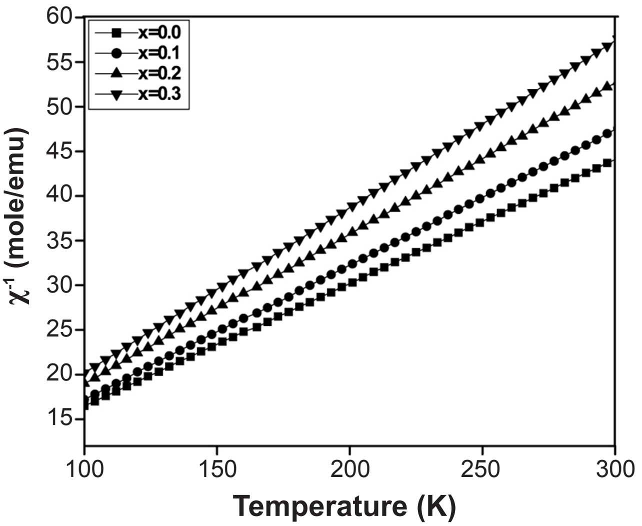

Figure 10: Inverse magnetic susceptibility as a function of the absolute temperature.
[Figure 10: Inverso da susceptibilidade magnética em função da temperatura absoluta.]

Using equations (D) and (E), the Curie constant and Bohr magneton number are obtained for each sample and listed in Table II. The Bohr magneton number obtained for Gd is $\mu_{eff} = 7.62\ \mu_B$ which is in good agreement with the reported literature [9] and theoretical value of $\mu_{eff} = 7.94\ \mu_B$.

It can be seen from the table II that Bohr magneton number is decreasing with increasing Pr concentration. This shows that the magnetic pair breaking phenomenon is responsible for destruction of superconductivity i.e. the magnetic order of $Gd_{1-x}Pr_xBa_2Cu_3O_{7-\delta}$ is suppressed by Pr substitution. This reflects that the magnetic interaction in Gd and Pr are probably different in nature. Our experimental results strongly confirm that magnetic pair breaking mechanism

Table II - Curie Constant, Bohr magneton number of $Gd_{1-x}Pr_xBa_2Cu_3O_{7-\delta}$ system.
[Tabela II - Constante de Curie, número do magneto de Bohr em $Gd_{1-x}Pr_xBa_2Cu_3O_{7-\delta}$*.]*

Pr conc.	C (K emu/mole)	μ_{eff} (μ_B) Experimental	μ_{eff} (μ_B) Calculated
0.0	7.20	7.62	7.94
0.1	6.59	7.29	7.62
0.2	5.96	6.93	7.28
0.3	5.40	6.60	6.93

is responsible for the destruction of superconductivity in Pr substituted Gd-123 samples. Thus one can say that in $Gd_{1-x}Pr_xBa_2Cu_3O_{7-\delta}$ system, the magnetic interaction in Gd and Pr cannot be neglected otherwise superconductivity would not be depressed.

CONCLUSIONS

Samples with chemical composition $Gd_{1-x}Pr_xBa_2Cu_3O_{7-\delta}$ were synthesized by ceramic route. All samples show orthorhombic pervoskite structure. Oxygen content depends on the lattice parameter 'c' and is almost independent on Pr content. The charge on $[Cu\text{-}O]^{+p}$ plane is dependent upon the combined effect of Pr concentration as well as oxygen content. The destruction of superconductivity by Pr substitution can be interpreted by means of increasing oxygen deficiency in the system. The value observed for $n(CuO_2)$ for optimum doping is 0.24. It implies that suppression of superconductivity results from a reduced number of carriers in the CuO_2 sheets and magnetic pair breaking effect. The decrement of T_C with increasing Pr concentration shows that the Pr concentration, carrier concentration and T_C are closely related to each other. It is also observed that the depression of T_C in Gd-123 is stronger than YPr-123. This may be due to the exchange interaction strengthened between hybridization of Pr and Gd 4f electrons because ionic radius of Gd^{3+} is larger than Y^{3+}. In $Gd_{1-x}Pr_xBa_2Cu_3O_{7-\delta}$ system, the magnetic order is suppressed by Pr substitution and the magnetic interaction in Gd and Pr cannot be neglected for destruction of superconductivity. The destruction of superconductivity in Pr substituted Gd-123 samples is owing to higher values of μ_{eff}.

ACKNOWLEDGEMENTS

Authors would like to thank University Grants Commission, New Delhi, for financial support through project F-37-563/2009/SR, Dr. S. K. Dhar, Tata Institute of Fundamental Research, Mumbai, for SQUID facilities, and Prof. S. S. Shah for encouragement.

REFERENCES

[1] M. Akhavan, Physica C **250** (1995) 25.

[2] M. Akhavan, Physica B **321** (2002) 265.

[3] R. Beyers, G. Lim, E. M. Engler, R. J. Savoy, T. M. Shaw, T. R. Dinger, W. T. Gallagher, R. L. Sandstom, Appl. Phys. Lett. **50** (1987) 1918.

[4] H. A. Blacksted, J. D. Dow, Phys. Rev. B **51** (1995)11830.

[5] H. A. Blackstead, J. D. Dow, D. B. Chrisey, J. S. Horwitz, M. A. Black, P. J. McGinn, A. E. Klunzinger, D. P. Pulling, Phys. Rev. B **54** (1996) 6122.

[6] C. H. Booth, F. Bridges, J. B. Boyee, T. Claeson, Z. X. Zhao, P. Cervantes, Phys. Rev. B **49** (1994) 3432.

[7] R. Buhleier, S. D. Brorson, I. E. Trifimo, J. O. White, H. U. Habermeier, J. Kuhl, Phys. Rev. B **50** (1994) 9672.

[8] R. J. Cava, A. W. Hewet, E. A. Hewet, B. Batlogg, M. Marezio, K. M. Rabe, J. J. Krajewski, W. F. Peck Jr, L. W. Rupp Jr, Physica C **165** (1990) 419.

[9] C. Chaillout, M. A. Alario-Franco, J. J. Capponi, J. Chenavas, P. Strobel, M. Marezio, Sol. State Comm. **65** (1988) 283.

[10] Y. Dalichaouch, M. S. Torikachvili, E. A. Early, B. W. Lee, C. L. Seaman, K. N. Yang, H. Zhou, M. B. Maple, Sol. State Comm. **65** (1988) 1001.

[11] B. N. Dole, S. S. Shah, Ind. J. Pur. Appl. Phys. **43** (2005) 279.

[12] R. Fehrenbacher, T. M. Rice, Phys. Rev. Lett. **70** (1993) 3471.

[13] R. M. Fleming, L. F. Schneemeyer, P. K. Gallagher, B. Batlogg, L. W. Rupp, J. V. Waszczak, Phys. Rev. B **37** (1988) 7920.

[14] W. Guan, Chin. J. Phys. 31 (1993) 849.

[15] W. Guan, Y. Xu, S. R. Sheen, Y. C. Chen, J. Y. T. Wei, H. F. Lai, M. K. Wu, Phys. Rev. B **49** (1994) 15993.

[16] P. Hor, R. L. Meng, Y. Qu Wang, L. Gao, Z. J. Huang, J. Bechtold, K. Forster, C. W. Chu, Phys. Rev. Lett. **58** (1987) 1891.

[17] C. S. Jee, A. Kebede, D. Nichols, J. E. Crow, T. Mihalisin, G. H. Myer, I. Perez, R. E. Salomon, P. Schlottman, Sol. State Comm. 69 (1989) 379.

[18] J. D. Jorgenson, M. A. Beno, D. G. Hinks, L. Solderholm, K. J. Volin, R. L. Hittermann, J. D. Grace, I. K. Schuller, C. U. Segre, K. Zhang, M. S. Kieefisch, Phys. Rev. B **36** (1987) 3608.

[19] J. D. Jorgenson, S. Pei, P. Lightfoot, H. Shi, A. P. Paulikas, B. W. Veal, Physica C **167** (1990) 571.

[20] J. Jung, M. A. K. Mohamed, S. C. Cheng, J. P. Franck, Phys. Rev. B **42** (1990) 6181.

[21] K. Kadowaki, Y. K. Huang, M. Van Sprang, A. A. Menovsky, Physica B **145** (1987) 1.

[22] H. Khosroabadi, V. Daadmehr, M. Akhavan, Mod. Phys. Lett. B **16** (2002) 943.

[23] J. K. Liang, S. S. Xie, H. G. Rao, X. Y. Shao, Z. G. Duan, Z. Phys. B **69** (1987) 137.

[24] S. Martin, A. T. Fiory, R. M. Fleming, L. F. Schneemeyer, J. V. Waszezak, Phys. Rev. Lett. **60** (1988) 2194.

[25] P. Monad, M. Ribault, F. D. Yvoire, J. Jegoudez, G. Collin, A. Revcolevschi, J. Phys. (Paris) **48** (1987)1369.

[26] J. J. Neumeier, T. Bjornholm, M. B. Maple, J. J. Rhyne, J. A. Gottas, Physica C **166** (1990) 191.

[27] B. Okai, M. Kosuge, H. Nozaki, T. Takahashi, M. Ohta, Jpn. J. Appl. Phys. **27** (1988) L41.

[28] H. B. Radousky, J. Mater. Res. **7** (1992) 1917.

[29] C. L. Seaman, J. J. Neumeier, M. B. Maple, L. P. Le, G. M. Luke, B. G. Sternlieb, Y. J. Uemura, J. H. Brewer, R. Kadono, R. F. Kiefl, S. R. Krietzman, T. M. Riseman, Phys. Rev. B **42** (1990) 6801.

[30] L. Solderholm, K. Zhang, D. G. Hinks, M. A. Beno, J. D. Jorgenson, C. U. Segre, I. K. Schuller, Nature **328** (1987) 604.

[31] S. Tanaka, Y. Motoi, Phys. Rev. B **52** (1995) 85.

[32] J. M. Tarascon, W. R. McKinnon, L. H. Greene, G. W. Hull, E. M. Vogel, Phys. Rev. B **36** (1987) 226.

[33] Y. Tokura, J. B. Torrance, T. C. Huang, A. I. Nazzal, Phys. Rev. B **38** (1988) 7156.
[34] Y. Xu, W. Guan, Physica C **183** (1991) 105.
[35] H. D. Yang, P. F. Chen, C. R. Hsu, C. W. Lee, C. L. Li, C. C. Peng, Phys. Rev. B **43** (1991) 10568.
[36] Z. Yamani, M. Akhavan, Physica C **268** (1996) 78.
[37] Z. Yamani, M. Akhavan, Supercond. Sci. Technol. **10** (1997) 427.
[38] Z. Yamani, M. Akhavan, Phys. Stat. Sol. A **163** (1997) 157.

(Rec. 17/10/2011, Rev. 26/03/2012, Ac. 30/03/2012)